Cerebral Cortex, 2018; 1–11

doi: 10.1093/cercor/bhx360
Original Article

ORIGINAL ARTICLE

Lack of Methyl-CpG Binding Protein 2 (MeCP2) Affects Cell Fate Refinement During Embryonic Cortical Development

Clementina Cobolli Gigli[1,5], Linda Scaramuzza[1], Marco De Simone[2], Riccardo L. Rossi[2], Davide Pozzi[3], Massimiliano Pagani[2], Nicoletta Landsberger[4,1] and Francesco Bedogni[1]

[1]San Raffaele Rett Research Unit, Division of Neuroscience, San Raffaele Hospital, 20132 Milan, Italy, [2]Istituto Nazionale Genetica Molecolare "Romeo ed Enrica Invernizzi", 20122 Milan, Italy, [3]Laboratory of Pharmacology and Brain Pathology, IRCCS Humanitas, 20089 Rozzano (MI) and Hunimed University, 20090 Pieve Emanuele (MI), Italy, [4]Department of Medical Biotechnology and Translational Medicine, University of Milan, 20090 Segrate, Milan, Italy and [5]Present address: Francis Crick Institute, 1 Midland Rd, Kings Cross, London NW1 1AT, UK

Address correspondence to Francesco Bedogni. Email: bedogni.francesco@hsr.it; Nicoletta Landsberger. Email: nicoletta.landsberger@unimi.it

Abstract

During differentiation, neurons progressively restrict their fate repressing the expression of specific genes. Here we describe the involvement in such developmental steps of the methyl-CpG binding protein 2 (MeCP2), an epigenetic factor that participates to chromatin folding and transcriptional regulation. We previously reported that, due to transcriptional impairments, the maturation of *Mecp2* null neurons is delayed. To evaluate whether this could stem from altered progenitors proliferation and differentiation, we investigated whether lack of Mecp2 affects these features both in vitro and in vivo. We show that in *Mecp2* null embryonic cortexes the expression of genes defining the identity of proliferating neuroprogenitors is enriched and that their permanence in the G1 phase is prolonged. Moreover, the number of cells transitioning from a stage of maturation to a more mature one is increased in *Mecp2* null embryonic cortices, in line with the central role of G1 for cell identity refinement. We thus suggest that, possibly due to the lack of proper transcriptional control normally exerted by Mecp2, fate refinement is impaired in developing null cells. We propose that the maturation delay affecting the developing *Mecp2* null cortex originates, at least in part, from deranged mechanisms of cell fate refinement.

Key words: cerebral cortex, differentiation, fate commitment, Mecp2, Rett syndrome

Introduction

Mutations of the X chromosome linked gene *MECP2* generate a plethora of different neurological disorders within which Rett syndrome (RTT) is the most strongly correlated (Amir et al. 1999; Tsankova et al. 2007; Diaz de Leon-Guerrero et al. 2011; Piton et al. 2011). RTT is a neurodevelopmental disease that affects mostly females; the onset of overt clinical symptoms is typically delayed and the pathology becomes evident after an initial early postnatal phase that has long been considered normal. Due to this feature, the field of RTT studies mostly investigated the roles played by methyl-CpG binding protein 2 (MeCP2) in adulthood (Pohodich and Zoghbi 2015). However, many studies now demonstrate that MeCP2 functions are important also during neuronal maturation. In fact, according

to retrospective analyses observations collected during the first few months of presymptomatic phase, RTT patients already display several subtle behavioral abnormalities (Nomura 2005; Fehr et al. 2011). Moreover, reduced occipitofrontal circumference, length, and weight are already present at birth (Huppke et al. 2003). Furthermore, the very rare cases of RTT male patients usually manifest harsh signs of neurological dysfunction already at birth, suggesting the onset of abnormalities already during embryonic development (Smeets et al. 2012). Interestingly, *Mecp2* animal models display structural and functional defects well before the overt symptomatic phase arises (Dani et al. 2005; Picker et al. 2006; Chao et al. 2007; Baj et al. 2014). Based on such indications, a new trend in MeCP2 studies is now analyzing its role during in vitro differentiation of stem cells (embryonic stem cells, neuronal stem cells, induced pluripotent stem cells). Such studies demonstrate that in vitro differentiated newborn null neurons display defects that largely overlap with features typically displayed by adult null neurons (Tsujimura et al. 2009; Marchetto et al. 2010; Okabe et al. 2010; Kim et al. 2011; Tanaka et al. 2014; Djuric et al. 2015). Accordingly, we have recently demonstrated that in vivo early differentiation is also altered, as the transcriptional profile of the E15.5 *Mecp2* null cortexes already display a decreased expression of genes defining the postmitotic identity of cortical glutamatergic neurons (Bedogni et al. 2016).

Taken together, these data suggest that MeCP2 concurs to early neuronal maturation and feasibly plays a role during the first phases of neurogenesis, when neural progenitor cells (NPCs) are proliferating and early neurons are being produced. Supporting this hypothesis, short interfering RNAs directed towards *MECP2* hamper proliferation in a number of non-neuronal cell types such as glial cells (Nagai et al. 2005), prostate cells and cancer prostate cells (Bernard et al. 2006), NIH/3T3 (Babbio et al. 2012), MEF and MRC5 (Bergo et al. 2015). Li and colleagues showed that Mecp2 plays a role also in the proliferation of neuronal precursors in adulthood. Mutation of the phosphorylation site S421 in fact reduces proliferation and increases differentiation of adult NPCs, thus, affecting the mechanisms that shape the fate they acquire (Li et al. 2014). Moreover, Mecp2 overexpression in the neural tube of chick embryos reduces the number of cycling cells while driving the premature differentiation of neurons ectopically positioned close to the ventricle (Petazzi et al. 2014). Finally, our transcriptional analysis of E15.5 cortexes showed that, beside the reduced expression of postmitotic genes, *Mecp2* null embryonic cortexes display increased levels of transcripts usually expressed by progenitors and early postmitotic neurons (Bedogni et al. 2016). These last results constitute the rationale of the present study. In Bedogni et al. (2016) we mostly focused on postmitotic maturation; in the present work, we investigate, in vitro and in vivo, whether cell cycle dynamics and cell fate decision are affected in *Mecp2* null NPCs. Our data suggest that, during neuronal differentiation, lack of *Mecp2* protracts the expression of genes that would normally be withdrawn to enable the refinement of the subsequent differentiation steps.

Materials and Methods

Animals and Tissues

The *Mecp2* mouse strain was purchased from Jackson Laboratories (B6.129P2(C)-Mecp2$^{<tm1.1Bird>/J}$) and transferred to a CD1 background (Cobolli Gigli et al. 2016). Genotypes were assessed as already described (Cobolli Gigli et al. 2016).

Time pregnant females were generated by crossing wild type (wt) males with *Mecp2* heterozygous (–/+) females, the day of vaginal plug was considered E0.5; embryos were then collected from anesthetized (Avertin, Sigma Aldrich) pregnant females. Embryos dedicated to histology were perfused with 4% paraformaldehyde (PFA) under a dissection microscope, post fixed for 4 h, cryoprotected at 4 °C in 30% sucrose, embedded in optimal cutting temperature (OCT) and sectioned in 12 μm frozen sections. Alternatively, embryos were fixed for 3 h at room temperature in 70% ethanol, 20% chloroform, 10% acetic acid, transferred in 100% ethanol, paraffin embedded and cut into 8 μm thick sections.

Time pregnant females were intraperitoneally injected at E15.5 with 5-ethynyl-2′-deoxyuridine (EdU; 30 mg/kg); embryos were collected 1 h later.

Ai27-NeuroD6-CRE double positive male mice (Jackson Laboratory) (Goebbels et al. 2006) were crossed with *Mecp2* heterozygous females to generate *Mecp2* null and wt mice expressing tdTomato in neurons.

All procedures were performed in accordance with the European Community Council Directive 86/609/EEC for care and use of experimental animals; all the protocols were approved by the Italian Minister for Scientific Research and by the local Animal Care Committee.

Neurospheres Generation

The generation of E15.5 NPCs cultures was described in Gritti et al. (1996). Briefly, dissected cortexes were transferred in Dulbecco's Modified Eagle Medium/F12 (DMEM/F12) and dissociated with Papaine (Sigma) and DNase (Roche). Cells were then grown in complete medium: DMEM/F12, 0.66% glucose, 2 mM L-glutamine, 1× Pen/Strep, 4 ng/ml heparin, hormone mix (DMEM/F12, glucose 0.06%, insulin 25 μg/ml, putrescine 9.7 μg/ml, apotransferrin 0.1 mg/ml, sodium selenite 0.03 μM, progesteron 0.02 μM), 20 ng/ml epidermal growth factor (EGF), 10 ng/ml basic fibroblast growth factor (bFGF); all such reagents were purchased from Sigma or Peprotech (EGF and bFGF). Spontaneously formed neurospheres were then dissociated in single cell cultures, plated on matrigel-coated coverslips and fixed with 4% PFA for microscopy.

For the 5-bromo-2′deoxyuridine (BrdU) incorporation assay, BrdU (10 μM, Sigma) was added to the culture every 2 h (for 14 h), at least 3 slides were collected 30 min after each administration.

For the neurospheres generation assay 5000 single cells were resuspended in 100 μl of complete medium in each well of a 96-well plate; the day of plating was considered DIV0. At DIV3 and 7 the generation of spheres was evaluated using an IN-Cell Analyzer 1000 System (GE Healthcare).

Histology, Immunofluorescence, and Immunohistochemistry

Mounted sections were washed in PBS and PBST (0.01% Tween20, Sigma) and incubated for 1 h in blocking solution (10% horse serum, 0.1% TritonX-100, PBS). When needed, antigen retrieval was achieved by heat treating in 0.01 M sodium citrate buffer (pH 6.4) and washing for 30 min in 0.1 M glycine (Sigma). BrdU detection required the incubation in 1 N chloric acid at 37 °C for 30 min. Tissues were then incubated overnight at 4 °C with the primary antibody diluted in blocking solution. Figure S1 describes primary antibodies concentrations and whether antigen retrieval was used. Slides were then thoroughly

washed in PBS, incubated for 1 h in Alexafluor secondary antibodies (Molecular Probes; 1:500 in blocking solution). For bright field imaging, biotinylated secondary antibody (Vector Laboratory) incubation was followed by signal amplification (ABC kit, Vector Laboratory); VIP peroxidase substrate (Vector Laboratory) was then used to produce the staining. Slides were mounted in Fluoromount-G (eBioscience) after incubation in DAPI (Invitrogen) and PBS washings. Tissues fixed in ethanol were handled in the same way after rehydration in xylene and decreasing ethanol solutions (100%, 75%, 50%). EdU detection required the Click-iT EdU Alexa Fluor 555 Imaging Kit.

Imaging was based on either a Leica TCS SP5 laser scanning confocal microscope (for histology) or a Zeiss Axio Imager II fluorescent widefield microscope (for cytological assessments). Cells were counted within bins of 50 μm × 330 μm by an investigator blinded to the experimental groups. Adobe Photoshop was used to either keep track of cell counts or build the panels for each regular and Supplementary figure. CyclinD1 intensity assessments required setting 3 different levels of threshold (weak, intermediate, strong; ImageJ) and manual counting. Dotted PCNA cells were counted applying a mask that automatically highlighted highly intense pixels (dots); cells containing dots were then manually counted. The number of single positive cells in Figure 4 refers to the number of cells expressing the single marker (Pax6, Tbr2) minus the number of cells expressing both markers (Pax6/Tbr2).

Two-way ANOVA comparing the distribution in each bin and the genotypes as variables and their interaction was used to analyze the statistical significance of our counts. Post hoc analysis, when needed, were based on Bonferroni's test, the confidence interval threshold (a) was set at 0.05. Values for each statistical assessment are described in figure legends.

Cell Sorting, RNA Purification, cDNA Synthesis, and Quantitative PCR

TdTomato positive embryos were produced by crossing Ai27 positive animals with NeuroD6 CRE drivers (Goebbels et al. 2006); recombination events were comparable in wt and Mecp2 null animals (Fig. S2). Tissues were dissected in HBSS and genotyped. Tissues were digested with Papaine (Sigma) and DNAse (Roche); cells were then sorted using FACSAria II (BD Bioscience) and collected in RNA later (Ambion). RNA was purified from TdTomato positive and negative wt and *Mecp2* null E15.5 embryos using the Nucleospin RNA XS RNA purification kit (Macherey-Nagel), eluted in 10 μl RNA/DNAse free H_2O and quality checked using a Bioanalyzer RNA 6000 Nano chips (Agilent). For qPCR experiments, 50 ng of total RNA were reverse-transcribed using Superscript IV Reverse Transcriptase (Thermo Fisher). For each sample, 1 ng of cDNA was preamplified using a 0.2X pool of 32 primers (TaqMan; including housekeeping, see Fig. S3) for 18 cycles using PreAmp Master Mix (Fluidigm) to enable multiplex sequence-specific amplification of targets. Preamplified cDNA was then diluted and assessed using the 96 × 96 qPCR DynamicArray microfluidic chips (Fluidigm) following the manufacturer's instructions. Baseline correction was set on Linear (Derivative), Ct Threshold Method was set on Auto (global) and Ct calculations were then elaborated in Excel (Microsoft). To normalize Ct, the stability of different housekeeping genes was calculated (NormFinder). All the values ranged between 0.010 and 0.018; PPia (0.016) was chosen as normalizer of all the transcriptional assessments.

Gene Set Enrichment Analysis

The gene set enrichment analysis (GSEA) (Subramanian et al. 2005) was performed on already published microarray data (Bedogni et al. 2016). We superimposed on this dataset 2 custom made gene-sets representing apical and basal progenitors (AP and BP) (Fig. S5) designed according to Telley et al. (2016).

Results

We previously demonstrated that embryonic cortexes lacking Mecp2 display increased levels of proliferative genes and, complementary, reduced expression of postmitotic transcripts, a phenotype that we interpreted as driven by a delay in maturation (Bedogni et al. 2016). Given that the acquirement of proper neuronal features and the establishment of mature cortical networks strictly depend on the dynamics of neuroprogenitors (NPCs) proliferation (Arai and Pierani 2014), we analyzed such dynamics in deeper details.

To this aim, we at first used in vitro cultures of cortical NPCs generated from E15.5 embryonic cortex. NPCs spontaneously proliferate forming neurospheres when cultured in the presence of mitogens (EGF and bFGF), (Gritti et al. 1996). Size and number of *Mecp2* null neurospheres in *Mecp2* null samples were comparable to controls at both early (day in vitro 3; DIV3) and late (DIV 7) stages of growth, in line with a previous study performing this analysis at DIV9 (Kishi and Macklis 2004) (Fig. 1*A*,*B*). This is in accordance with previous reports proposing that Mecp2 deficiency does not compromise neurogenesis; many studies in fact point out that the number of neurons populating the adult *Mecp2* null cortex is comparable to wt (Chen et al. 2001; Guy et al. 2001; Kishi and Macklis 2004). However, with this approach we could not exclude subtle alterations in the cell cycle dynamics. To further assess whether cell cycle progression of *Mecp2* null NPCs could be affected, we analyzed the rate of BrdU incorporation within a short time window. To avoid any influence driven by disparities in cell density, we plated cortical progenitors obtained from *Mecp2* heterozygous females. Given Mecp2 is an X chromosome linked gene, in heterozygote samples, after random X chromosome inactivation, each cell expresses either the wt or the *Mecp2* null allele. The expression of Mecp2 was assessed post hoc using a specific antibody (Fig. 1*C*). Plated NPCs were cultured in proliferating conditions, BrdU (10 μM) was added every 2 h and samples were collected 30 min after each BrdU administration (Fig. 1*D*). The experiment lasted 14.5 h, thus less than an entire cell cycle (Takahashi et al. 1995). In line with the neurosphere formation assay, both Mecp2 positive and negative cells reached a plateau stage, implying that both types of cells eventually entered cell cycle. However, 2.5 h after the first BrdU addition, the proportion of negative cells incorporating BrdU was reduced by roughly 20%, suggesting that Mecp2 absence reduces the number of cells in S phase.

A possible drawback of these in vitro assessments might be the lack of extracellular cues participating to the regulation of cell cycle progression; we thus assessed cell cycle progression in vivo. To identify the proliferative compartment, we performed immunostainings of cortices at E15.5 using specific antibodies. As depicted in Figure S4, cells positive for specific cell cycle antigens were counted in the innermost bins of the grid we used to subdivide the cortical thickness (see Materials and Methods for details). To identify the bins corresponding to the proliferative compartment we evaluated, in wt conditions, the position of cells expressing the pan cell cycle related protein

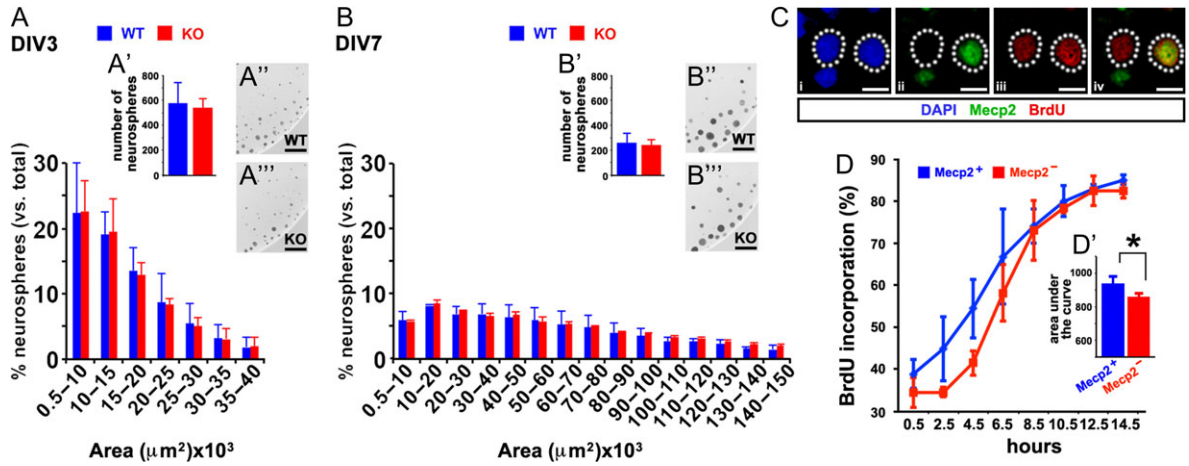

Figure 1. Mecp2 concurs, in vitro, to the dynamics of NPCs proliferation. (*A*, *B*) Wt and *Mecp2* null NPCs, cultivated in vitro in proliferating conditions, produce neurospheres of comparable size at both 3 (*A*, *A*″, *A*‴) and 7 DIV (*B*, *B*″, *B*‴). The number of neurospheres produced is accordingly equal (*A*′, *B*′). Values represent the mean (± standard deviation) of 3 independent determinations; each determination was assessed on a pool of NPCs deriving from at least 3 different *Mecp2* null and wt animals. Statistical analysis: Student's *t* test, no significant values. Scale bar: *A*″, *A*‴, *B*″, *B*‴: 500 μm. (*C*, *D*) BrdU was administered each 2 h to heterozygous NPCs, cultured as an adherent monolayer in proliferating conditions. The percentage of BrdU positive cells (over the total counted) is depicted in *C*; values represent the mean (± standard deviation) of 3 different neurosphere preparations. Scale bar: i, ii, iii, iv: 10 μm. The percentage of BrdU stained cells either positive or negative for Mecp2 expression was plotted in *D* (±standard deviation) and the area under the curve was calculated to assess the statistical significance of the difference in the rate of BrdU incorporation (*D*′, Student *t*-test).

Ki67 (Fig. S4A, C; Turrero Garcia et al. 2016) which were abundant in the first 2 bins, slightly reduced in bins 3 and 4 and only rarely detected in bins 5 and 6 that are mostly populated by cells expressing the neuronal marker NeuN (Mullen et al. 1992). Bins 1–4 thus coincide with the proliferative compartment and were therefore the main focus of cell cycle dynamic assessments.

To assess S phase, E15.5 pregnant *Mecp2* heterozygote females were injected with EdU (30 mg/kg, Fig. 2A) 1 h before embryos collection and the number of positive cells was counted in wt and *Mecp2* null male embryos. As depicted in Figure 2D, the number of EdU positive cells in null cortexes was similar to that of wt samples as overall number and within each bin. The progression through the subsequent cell cycle phases was assessed discriminating between dotted or solid phospho-histone H3 (PH3) staining to recognize cells in G2 or M phase, respectively (Hendzel et al. 1997; Van Hooser et al. 1998). Our counts did not highlight any variation in the number of positive cells (Fig. 2E,F). We thus concluded that the progression of null progenitors through S, G2, and M phases resulted for the most part unaffected.

We completed this analysis by considering the transition through G1 using CyclinD1 (Baldin et al. 1993). In line with the fact that the length of the G1 phase at E15.5 is much larger compared with the others (Takahashi et al. 1995; Arai et al. 2011), CyclinD1 positive cells were more abundant compared with those transitioning through S, G2, and M in both wt and *Mecp2* null samples (Fig. 2C,G). Although our counts did not reveal any difference in the total number of CyclinD1 positive progenitors populating the wt or the null cortexes (Fig. 2G), the analysis of the number of positive cells in each bin revealed particularly intriguing, as two-way ANOVA revealed a *P* value of 0.037 for the interaction between genotypes and bins subdivision. Moreover, a significantly increased number of CyclinD1 positive cells (P value of 0.0208, Bonferroni post hoc test; Fig. 2G′) was detected in bin 3, an area that roughly coincides with the subventricular zone (SVZ; as in Fig. S4A, E). Based on this evidence, we next proceeded with a more detailed analysis of the G1 phase. As depicted in Figure 2C, the intensity of CyclinD1 signal varied from cell to cell regardless their positioning within the proliferative compartment. It was in fact possible to set thresholds to recognize cells expressing strong, intermediate or weak levels of it (Fig. 3A), which in wt samples represented the 13%, 40%, and 46% (standard deviation: ±3.08, ±2.88, and ±4.58, respectively) over the total counted. Intriguingly, we detected a significant increased number of weakly CyclinD1 positive cells in bins 2, 3, and 4 (Fig. 3B; two-way ANOVA followed by Bonferroni's post hoc test). The levels of CyclinD1 are important for S phase entrance, as CyclinD1 overexpression shortens the length of the G1 phase (Lange et al. 2009), while its inhibition slows G1/S transition (Calegari and Huttner 2003; Cremisi et al. 2003), thus implying that high levels of CyclinD1 are expressed by cells approaching the S phase. In line with this, our data demonstrated that in wt animals, cells exiting the M phase and entering in the G1 phase (recognized through solid PH3 and CyclinD1 double expression, Fig. 3C) express intermediate or weak levels of CyclinD1, as quantified in Figure 3D. Moreover, as predicted, cells entering the S phase (recognized by a dotted PCNA staining typical) (Arai et al. 2011) (Fig. 3E) express higher levels of CyclinD1 (Fig. 3F), thus in line with the role of high levels of CyclinD1 in driving S phase entrance. Together, this suggests that, compared with wt, the increased number of *Mecp2* null progenitors that express low levels of CyclinD1 likely reside in G1 for a prolonged amount of time.

Since G1 length is crucial for determining the fate each cell will acquire (Caviness et al. 2003; Lange et al. 2009), we next assessed whether the subsequent steps of neuronal differentiation were also affected. Cortical development relies on the tightly regulated (both in time and space) expression of a number of markers defining the level of maturity each cell type has reached (Molyneaux et al. 2007). In particular, Pax6 enables to recognize APs, thus progenitors that divide either symmetrically to produce 2 Pax6 positive cells or asymmetrically to produce either a postmitotic newborn neuron or a BP that expresses Tbr2 (Englund et al. 2005; Hevner et al. 2006; Florio and Huttner 2014). We focused, again, on the first 4 bins of the grid, as these cover the entire area in which both Pax6 and Tbr2

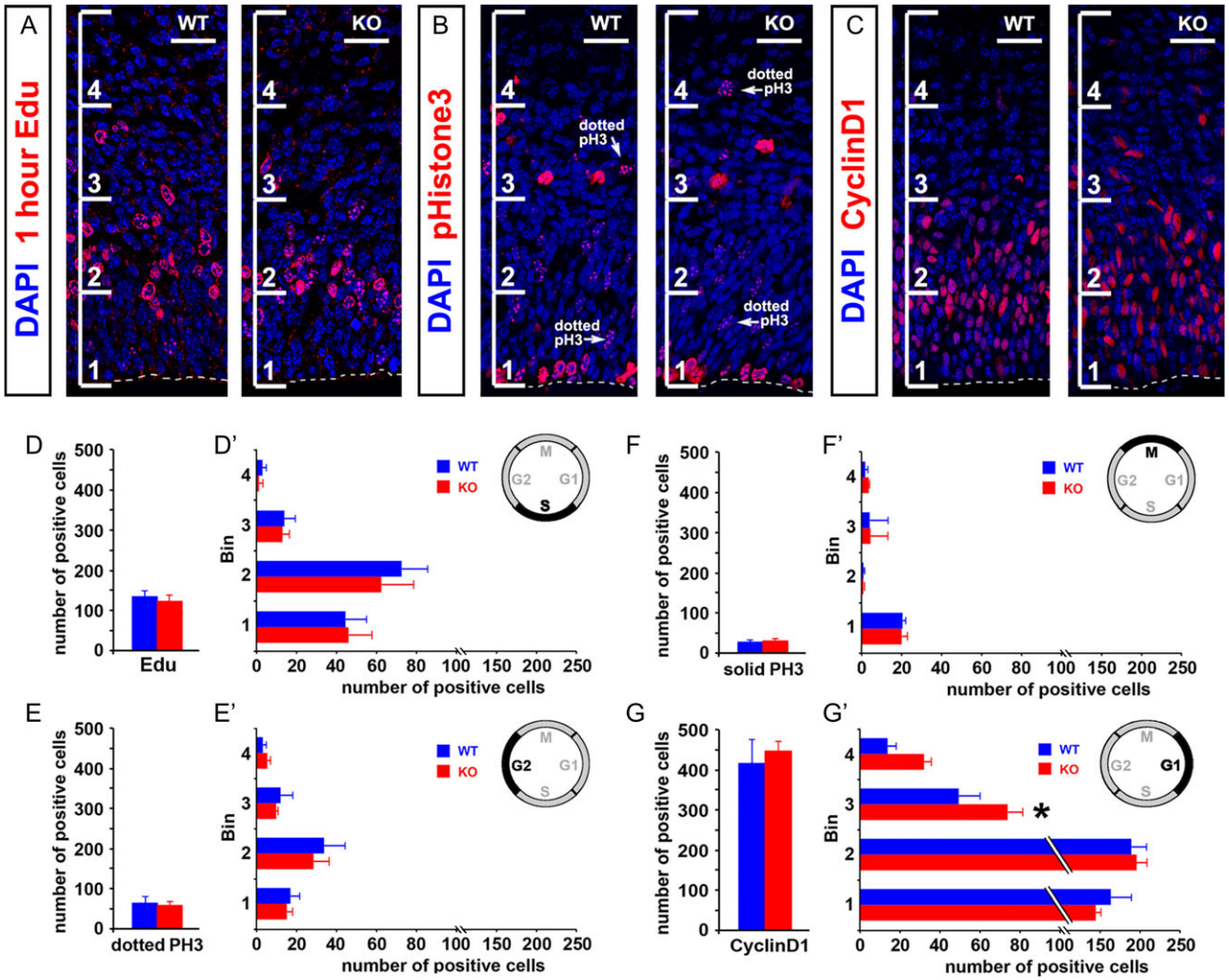

Figure 2. NPCs populating E15.5 *Mecp2* null cortexes normally progress through the S–G2–M phases of the cell cycle while the number of cells residing in the G1 phase of the cell cycle is increased. (*A–C*) Representative staining of the different markers used to recognize different cell cycle phases in wt and *Mecp2* null samples. Scale bar in *A*, *B*, *C*: 25 µm. (*D–D′*) The total number of EdU positive cells, representing cells in the S phase, was not different both between genotypes and in singly taken bins. Two-way ANOVA: interaction: $F = 2.123$, $P = 0.1023$. (*E–E′*) PH3 staining is dotted during the G2 phase. No changes were detected in either total positive numbers or within each bin. Two-way ANOVA: interaction: $F = 1.018$, $P = 0.3932$. (*F–F′*) Cells in M phase display a solid PH3 staining. No changes were detected in either total positive numbers or within each bin. Two-way ANOVA: interaction: $F = 0.3002$, $P = 0.8251$. (*G–G′*) CyclinD1 was used to highlight cells in G1. While total number were not different (*G*), the interaction between genotype and bin distribution (two-way ANOVA) was: $F = 5.124$, $P = 0.0037$ (*G′*). For bin 3, the post hoc Bonferroni's test *P* value was 0.0208. Values represent the mean (± standard deviation), $n = 16$ wt, 10 *Mecp2* null in *D*, *D′*, for all the rest: $n = 9$ wt, 6 *Mecp2* null.

positive cells are located (Fig. S4A, D, E). In particular, a larger percentage of Pax6 positive cells populate bins 1 and 2, which roughly coincides to the ventricular zone (VZ), while the distribution of Tbr2 positive cells is more spread in the 4 bins, with the majority of positive cells residing in bins 2 and 3 (roughly coinciding with SVZ). As depicted in Figure 4*A′*,*B′*, the total number of single positive cells expressing either Pax6 or Tbr2 did not differ between E15.5 wt and *Mecp2* null cortexes. However, we found an increased number of double positive cells both as total numbers (Fig. 4*D*) and within bins (Fig. 4*D′*; two-way ANOVA followed by post hoc Bonferroni test). Given Pax6 and Tbr2 are simultaneously expressed during the transition from one population to the other (i.e., from AP to BP), this result suggests that a larger number of cells transitioning from the apical to the basal identity populates the *Mecp2* null proliferative compartment. Accordingly, 2 gene-sets defining the AP and BP transcriptional identity (based on published data, (Telley et al. 2016)) superimposed on the transcriptional profile of E15.5 *Mecp2* null cortexes (previously described in Bedogni (Bedogni et al. 2016)) showed that such identities are both significantly enriched in null samples compared with wt (Fig. S5A, B, B′).

Next we asked whether Mecp2 absence might also affect the transcriptional changes occurring during the transition from the stage of progenitor to that of newborn neurons. Early postmitotic cells, in fact, progressively abandon their (obsolete) progenitor identity and, while migrating towards the cortical plate, refine their neuronal features (Hevner et al. 2006; Molyneaux et al. 2007).

To study in details the withdrawal of former transcriptional identities, we thus segregated progenitors and early postmitotic cells from fully matured neurons. To this aim we used a genetic approach based on the expression pattern of *NeuroD6*, a gene expressed by few cells in the VZ/SVZ and by each postmitotic neuron in the intermediate zone and the cortical plate (Fig. S6). Ai27-NeuroD6-CRE double transgenic males, in which tdTomato (tdT) expression is limited to postmitotic NeuroD6 positive

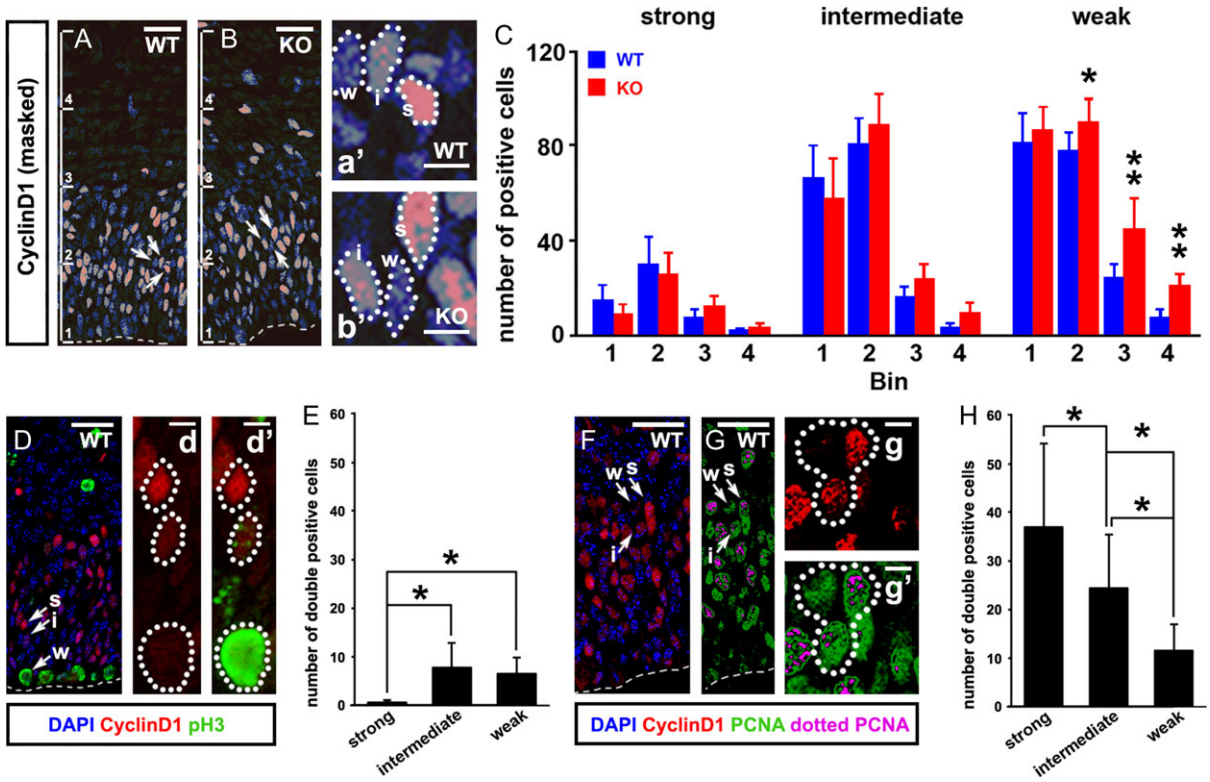

Figure 3. The number of cells residing in G1 phase is increased in *Mecp2* null cortexes. (*A*) CyclinD1 positive cells were analyzed in wt and *Mecp2* null samples according to the intensity of the signal (s: strong, i: intermediate, w: weak). (*B*) Quantitation of CyclinD1 positive cells in wt and *Mecp2* null samples according to the signal intensity. Two-way ANOVA for strong and intermediate stained cells: *F*: 2.212, *P* = 0.0977; *F*: 2.316, *P* = 0.0865. For weakly stained cells, after two-way ANOVA, the *P* values for the variables genotype and bin distribution were 0.0001 and 0.0001, respectively, *F* = 1.947, *P* = 0.1335. Bonferroni's post hoc test revealed that the *P* values for bins 2, 3, and 4 were 0.041, 0.0001, and 0.013, respectively. (*C*, *D*) CyclinD1 levels were evaluated in PH3 positive cells and quantified in *D* (± standard deviation; Student *t*-test). (*E*, *F*) CyclinD1 levels were evaluated in PCNA dotted cells and quantified in *H*. PCNA dots were evaluated through the use of an imageJ mask that highlight intense pixels, as depicted in e–e″′ and quantified in *F* (± standard deviation; Student *t*-test). Scale bar in a′, a″, c′, e′, e″: 25 µm; a″′, a″″, c″, c″′, e″′, e″″: 5 µm. *n* = 9 wt, 6 *Mecp2* null.

neurons, were crossed to *Mecp2* heterozygous females to produce wt and *Mecp2* null E15.5 cortexes bearing tdT$^+$ and tdT$^-$ cells. Both these populations were dissected out from E15.5 cortexes, FACS sorted (based on the fluorescent tdTomato signal) and analyzed through qPCR. Importantly, we verified that the expression of NeuroD6 does not change between wt and *Mecp2* null samples in E15.5 total cortical extracts and in both populations of sorted cells (tdT$^-$ and tdT$^+$, Fig. 5A); these results confirm that the number of generated neurons is not affected by lack of *Mecp2* (Kishi and Macklis 2004). In accordance with the expression pattern of *NeuroD6*, its levels were notably higher in the tdT$^+$ population compared with the tdT$^-$ (Fig. 5A). Intriguingly, Figure 5B demonstrates that some newborn neurons located within the VZ/SVZ expressing the early neuronal marker Tuj1 are not yet tdT$^+$. Given that at early stages of postmitotic differentiation the fluorescent signal could be too weak to ensure FACS collection in the tdT$^+$ pool (due to low expression of *NeuroD6* and, consequently, low activation of CRE), we speculated that the dtT$^-$ population included also cells transitioning from the stage of progenitors to newborn postmitotic neurons.

Next, we assessed the expression of a panel of genes that are typical of progenitors, postmitotic neurons or both. All qPCR amplifications were simultaneously run and normalized (based on housekeeping genes, see Materials and Methods), thus enabling to compare the levels of expression of each gene in the 2 different populations according to its normalized amplification curve (ΔCt). The Y-axis of Figure 5D shows the difference in the expression of each gene in the tdT$^-$ and tdT$^+$ samples (ΔCt of tdT$^-$ minus ΔCt of tdT$^+$): negative values corresponded to genes enriched in tdT$^-$, while genes enriched in tdT$^+$ had positive values. After ranking on the *X*-axis each gene according to such values, genes expressed in progenitors segregated from those of postmitotic neurons from left (higher expression in tdT$^-$) to right (higher expression in tdT$^+$) (Ayoub et al. 2011). Accordingly, *Mecp2* resides in the middle of these 2 extremes, given its expression is roughly equal in mitotic and postmitotic cells (Li et al. 2013; Bedogni et al. 2016). Altogether, these observations validated our sorting strategy.

Figure 5E–E′ refers to the transcriptional levels and pattern of expression of genes highly enriched in either the VZ/SVZ or intermediate zone (IZ, as depicted in Fig. S6). Our analysis demonstrated that within such genes, *Hes1, Tbr2, Ngn2* (all specifically expressed by cortical progenitors) resulted significantly upregulated in the tdT$^-$ population of the *Mecp2* null samples. Further, we tested genes expressed by either cells transitioning from the proliferative identity to the postmitotic one (*Rnd2, NeuroD1*) (Hevner et al. 2006; Heng et al. 2008) or postmitotic cells (*NeuN*). Compared with wt, their levels in *Mecp2* null samples resulted increased in tdT$^-$, although not in a significant way in the case of NeuN (*P* = 0.064). No differences in the expression levels of the genes analyzed were detected in tdT$^+$ (Fig. 5E′) likely due to the fact that this population is more differentiated compared with the one our sorting strategy meant to enrich.

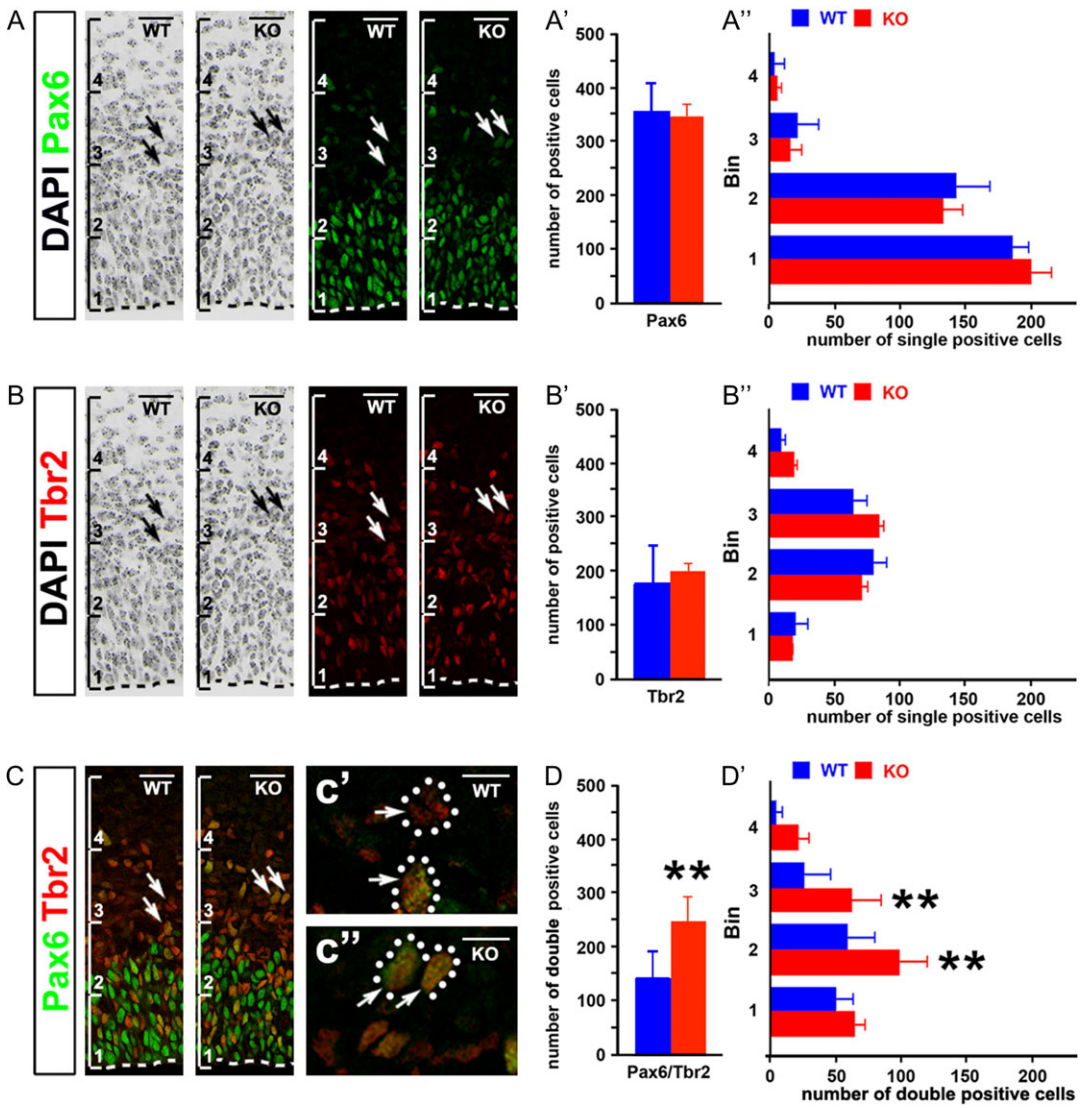

Figure 4. Mecp2 absence interferes with the transition from one identity, to the subsequent, more mature one. (*A*) The number of Pax6 positive cells (APs) was assessed as either total number (*A′*) or within bins (*A″*). (B) The number of Tbr2 positive cells (BPs) was assessed as either total number (*B′*) or within bins (*B″*). (*C*) Double positive cells were counted either as total number (*D*) or within bins (*D′*). The total number of double positive cells was significantly increased (*D*, Student *t*-test); two-way ANOVA of the analysis in *D′* revealed a $F = 2.281$ and $P = 0.0904$. Bonferroni's post hoc test in bin 2 and 3 revealed *P* values of 0.0001 and 0.0004, respectively. (*D*) Colocalization of Pax6 and Tbr2 in wt and null samples. Values represent the mean (± standard deviation). $n = 9$ wt, 6 *Mecp2* null. Scale bar for *A*, *B*, *C*: 25 μm; inserts in *D*: 10 μm.

The increased transcription of *NeuroD1* is of particular interest, as its expression is limited to a population of cells transitioning from the late phases of the cell cycle to the early steps of postmitotic maturation. Given our interest for the defects in the transition from one stage of development to a more mature one, we further investigated this result by counting the number of NeuroD1 positive cells in E14.5 wt and *Mecp2* null cortices (Fig. 5*F*). As depicted in Figure 5G, although the total levels of NeuroD1 positive cells were increased but not significantly ($P = 0.078$), the number of positive cells in the third bin (where the wide majority of positive cells are located) was significantly increased in *Mecp2* null samples compared with wt (130.7 vs. 161.4, standard deviation: ±18.3 and 16.1, respectively, two-way ANOVA followed by Bonferroni post hoc test). This is in line with our hypothesis of a delayed progression toward a more mature stage of differentiation affecting *Mecp2* null cortexes.

Discussion

The demonstration that Mecp2 plays a role during embryonic and early postnatal life has opened a new venue in RTT studies (Feldman et al. 2016). However, whether Mecp2 is involved in early phases of NPCs proliferation and differentiation is still an open question. The present study provides evidence of the involvement of Mecp2 in such stages, possibly linking impaired NPCs fate refinement to delayed cortical neurons maturation.

The 6-layered mature cerebral cortex arises from temporally and spatially regulated processes that begin with the establishment and the expansion of a pool of progenitor cells. Within this pool, APs express Pax6 and reside in the VZ where they divide symmetrically to self-regenerate or asymmetrical generating a new AP and either a newborn neuron or a BP (Haubensak et al. 2004; Miyata et al. 2004; Noctor et al. 2004).

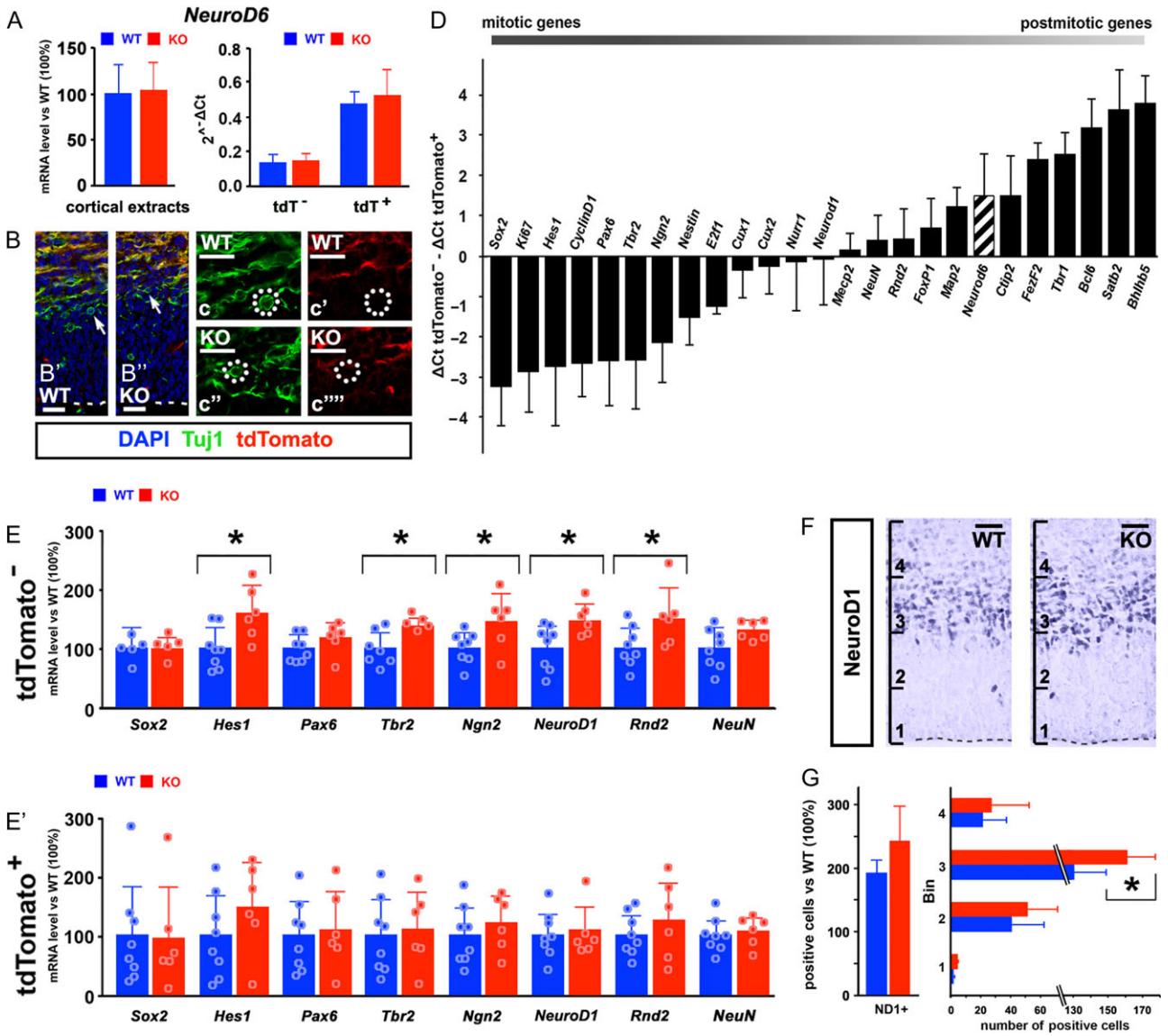

Figure 5. Genes expressed by either NPCs or cells transitioning to postmitotic stages of maturation are upregulated in null samples. (*A*) qPCR analyses of *NeuroD6* expression in wt and *Mecp2* null samples deriving from total cortical extracts (left) and tdT^{-} and tdT^{+} (right) samples, the relative expression was plotted as percentage compared with wt (100%) in the case of total extracts or as $2^{-\Delta Ct}$ in the case of the 2 sorted populations. (*B*) Tuj1 (neuronal marker) expression precedes the expression of tdTomato in both wt (*B′*) and null (*B″*) samples; all postmitotic neurons populating the IZ and the CP abundantly express both Tuj1 and tdT. Scale bars: *B′*, *B″*, c–c‴: 20 μm. (*D*) Genes expressed by different cortical populations in wt samples were ranked based on the difference obtained by subtracting the value of ΔCt of tdT^{+} from the value of the ΔCt of tdT^{-}. (*E*–*E′*) The expression level of 5 genes typically expressed by progenitors was evaluated in either tdT^{-} (*E*) or tdT^{+} (*E′*) populations. Each level was expressed as percentage of *Mecp2* null levels compared with wt (100%). Statistical analysis: Student's *t* test: *$P < 0.05$. Values represent the mean (± standard deviation); $n = 8$ wt, 6 *Mecp2* null samples. (*F*) Pattern of expression of NeuroD1 in wt and *Mecp2* null cortexes. Scale bars: 25 μm. (*G*) Quantitation of NeuroD1 positive cells within wt and *Mecp2* null samples. While the total number of positive cells was almost significantly increased ($P = 0.078$, *t*-test), after two-way ANOVA, the *P* values for the variables genotype and bin distribution were 0.0191 and <0.0001, respectively. The *F* and *P* values for interaction were 1.528 and 0.2239. Bonferroni post hoc test revealed a significant ($P = 0.0187$) increased in the number of positive cells in bin 3. Values represent the mean (± standard deviation); data were produced from a minimum of 5 different determinations per genotype.

Located in the SVZ, BPs express Tbr2 and symmetrically divide to generate either 2 new BPs or 2 neurons (Englund et al. 2005; Florio and Huttner 2014). The establishment of mature projection neurons thus requires the activation of specific transcriptional programs orchestrating the transition through each step of neurogenesis (Hevner et al. 2006; Molyneaux et al. 2007; Telley et al. 2016). Such mechanisms are regulated already at the level of cell cycle progression, as cells cycling to expand the progenitor pool have a longer S phase compared with those generating newborn neurons (Arai et al. 2011). Moreover, G1 progressively lengthens during neurogenesis, enabling cells to establish their next fate (including whether exiting or re-entering the cell cycle) by combining intrinsic differentiation programs with the increasing number of cues from the surrounding environment (Calegari and Huttner 2003; Lange et al. 2009; Hardwick et al. 2015). We show here that a larger number of CyclinD1 (marker of G1) positive cells populate the *Mecp2* null cortexes, thus implying that more cells reside in G1 and suggesting a delayed commitment. Accordingly, the number of transitioning cells (Pax6/Tbr2 double positive) is increased in

Mecp2 null cortexes. Moreover, in a population that likely contains such cells (tdTomato$^-$) the transcription of some general markers of either progenitors or cells transitioning towards postmitotic differentiation is increased in null samples. This suggests that null cells persistently express genes that, in wt conditions, would typically be withdrawn to enable fate refinement and maturation.

Epigenetic control of transcription is largely involved during maturation, when each cell restricts its fate by repressing the expression of specific genes (MacDonald and Roskams 2009; MuhChyi et al. 2013). Thus, we propose that the persistent transcription of key neurodevelopmental genes and the consequent presence of unrefined cellular types in *Mecp2* null samples should be considered under the light of the epigenetic role MeCP2 plays in repressing transcription (Bedogni et al. 2014; Lombardi et al. 2015). Supporting this hypothesis, Mecp2 absence affects the phenotypic refinement of newborn neurons in the adult hippocampal granular zone that shows an increased number of cells coexpressing Doublecortin (Dcx) and NeuN in *Mecp2* null animals (Smrt et al. 2007). Given NeuN positive neurons are considerably more mature compared with Dcx positive, the persistent expression of Dcx suggests a phenotype that largely overlaps with the one described here.

We are aware that previous studies in adult *Mecp2* null tissues predominantly highlighted transcriptional downregulations (Tudor et al. 2002; Kriaucionis et al. 2006; Chahrour et al. 2008; Ben-Shachar et al. 2009; Yazdani et al. 2012; Li et al. 2013); such unexpected evidence might originate from indirect effects such as compensatory mechanisms downgrading gene expression to dump the transcriptional noise driven by the absence of Mecp2. The levels of linker histone H1 are in fact increased in *Mecp2* null mature neuronal nuclei, likely as part of such compensatory mechanisms (Skene et al. 2010). We thus believe that the direct transcriptional consequences of Mecp2 deficiency are more evident at the stage of progenitors or newborn neurons, when compensatory mechanisms are not yet, or not fully, activated. However, the persistent expression in null neurons of genes that would typically be withdrawn in wt samples disappears at later time (Fig. 5E′), when such genes return to normal levels. Nonetheless, their deregulation during early stages of postmitotic cell refinement likely concurs to the transcriptional defects that in a previous study we interpreted as a delay in maturation (Bedogni et al. 2016). To conclude, we show a new embryonic role played by Mecp2 during critical steps of cell fate refinement. In null early born cortical neurons deranged fate refinement likely concurs to other transcriptional defects that include the reduced expression of transcripts mediating responsiveness to external stimuli and activity (Bedogni et al. 2016). Given activity is one of the main drivers of neuronal maturation and network establishment (Spitzer 2006), the integration of immature neurons in the developing cortical networks would consequently be further delayed, in line with the typical immaturity of adult *Mecp2* null neuronal networks (Dani et al. 2005; Lang et al. 2014). Overall, this study extends our knowledge over the role of MeCP2 during brain development and reinforces the rationale of therapeutic strategies promoting neuronal maturation (Tropea et al. 2009). Eventually, deranged mechanisms of early corticogenesis provide a framework not only for RTT but also for other neurological disorders originating from *MECP2* mutations (Tsankova et al. 2007; Neul 2012; Ernst 2016).

Supplementary Material

Supplementary material is available at *Cerebral Cortex* online.

Notes

The authors would like to thank doctors Vania Broccoli and Stefano Taverna for the generous gifts of the NeuroD6-CRE and Ai27 mice, respectively. Cell sorting was made possible thanks to the sorting facility at Humanitas Clinical and Research Center (Milan, Italy). All the imaging studies were made possible through the technical support offered by the team at the San Raffaele Microscopy Facility (ALEMBIC). We are grateful to ProRett Research, an association of RTT girls' parents providing us with both strive and funding to study RTT and Mecp2. The Lejeune Foundation (Paris, France) provided additional funding to FB. *Conflict of Interest*: None declared.

References

Amir RE, Van den Veyver IB, Wan M, Tran CQ, Francke U, Zoghbi HY. 1999. Rett syndrome is caused by mutations in X-linked MECP2, encoding methyl-CpG-binding protein 2. Nat Genet. 23:185–188.

Arai Y, Pierani A. 2014. Development and evolution of cortical fields. Neurosci Res. 86:66–76.

Arai Y, Pulvers JN, Haffner C, Schilling B, Nusslein I, Calegari F, Huttner WB. 2011. Neural stem and progenitor cells shorten S-phase on commitment to neuron production. Nat Commun. 2:154.

Ayoub AE, Oh S, Xie Y, Leng J, Cotney J, Dominguez MH, Noonan JP, Rakic P. 2011. Transcriptional programs in transient embryonic zones of the cerebral cortex defined by high-resolution mRNA sequencing. Proc Natl Acad Sci USA. 108:14950–14955.

Babbio F, Castiglioni I, Cassina C, Gariboldi MB, Pistore C, Magnani E, Badaracco G, Monti E, Bonapace IM. 2012. Knockdown of methyl CpG-binding protein 2 (MeCP2) causes alterations in cell proliferation and nuclear lamins expression in mammalian cells. BMC Cell Biol. 13:19.

Baj G, Patrizio A, Montalbano A, Sciancalepore M, Tongiorgi E. 2014. Developmental and maintenance defects in Rett syndrome neurons identified by a new mouse staging system in vitro. Front Cell Neurosci. 8:18.

Baldin V, Lukas J, Marcote MJ, Pagano M, Draetta G. 1993. Cyclin D1 is a nuclear protein required for cell cycle progression in G1. Genes Dev. 7:812–821.

Bedogni F, Cobolli Gigli C, Pozzi D, Rossi RL, Scaramuzza L, Rossetti G, Pagani M, Kilstrup-Nielsen C, Matteoli M, Landsberger N. 2016. Defects during Mecp2 null embryonic cortex development precede the onset of overt neurological symptoms. Cereb Cortex. 26:2517–2529.

Bedogni F, Rossi RL, Galli F, Cobolli Gigli C, Gandaglia A, Kilstrup-Nielsen C, Landsberger N. 2014. Rett syndrome and the urge of novel approaches to study MeCP2 functions and mechanisms of action. Neurosci Biobehav Rev. 46(Pt 2): 187–201.

Ben-Shachar S, Chahrour M, Thaller C, Shaw CA, Zoghbi HY. 2009. Mouse models of MeCP2 disorders share gene expression changes in the cerebellum and hypothalamus. Hum Mol Genet. 18:2431–2442.

Bergo A, Strollo M, Gai M, Barbiero I, Stefanelli G, Sertic S, Cobolli Gigli C, Di Cunto F, Kilstrup-Nielsen C, Landsberger N. 2015. Methyl-CpG binding protein 2 (MeCP2) localizes at the centrosome and is required for proper mitotic spindle organization. J Biol Chem. 290:3223–3237.

Bernard D, Gil J, Dumont P, Rizzo S, Monté D, Quatannens B, Hudson D, Visakorpi T, Fuks F, de Launoit Y. 2006. The

methyl-CpG-binding protein MECP2 is required for prostate cancer cell growth. Oncogene. 25(9):1358–1366.

Calegari F, Huttner WB. 2003. An inhibition of cyclin-dependent kinases that lengthens, but does not arrest, neuroepithelial cell cycle induces premature neurogenesis. J Cell Sci. 116: 4947–4955.

Caviness VS Jr, Goto T, Tarui T, Takahashi T, Bhide PG, Nowakowski RS. 2003. Cell output, cell cycle duration and neuronal specification: a model of integrated mechanisms of the neocortical proliferative process. Cereb Cortex. 13: 592–598.

Chahrour M, Jung SY, Shaw C, Zhou X, Wong ST, Qin J, Zoghbi HY. 2008. MeCP2, a key contributor to neurological disease, activates and represses transcription. Science. 320:1224–1229.

Chao HT, Zoghbi HY, Rosenmund C. 2007. MeCP2 controls excitatory synaptic strength by regulating glutamatergic synapse number. Neuron. 56:58–65.

Chen RZ, Akbarian S, Tudor M, Jaenisch R. 2001. Deficiency of methyl-CpG binding protein-2 in CNS neurons results in a Rett-like phenotype in mice. Nat Genet. 27:327–331.

Cobolli Gigli C, Scaramuzza L, Gandaglia A, Bellini E, Gabaglio M, Parolaro D, Kilstrup-Nielsen C, Landsberger N, Bedogni F. 2016. MeCP2 related studies benefit from the use of CD1 as genetic background. PLoS One. 11:e0153473.

Cremisi F, Philpott A, Ohnuma S. 2003. Cell cycle and cell fate interactions in neural development. Curr Opin Neurobiol. 13:26–33.

Dani VS, Chang Q, Maffei A, Turrigiano GG, Jaenisch R, Nelson SB. 2005. Reduced cortical activity due to a shift in the balance between excitation and inhibition in a mouse model of Rett syndrome. Proc Natl Acad Sci USA. 102: 12560–12565.

Diaz de Leon-Guerrero S, Pedraza-Alva G, Perez-Martinez L. 2011. In sickness and in health: the role of methyl-CpG binding protein 2 in the central nervous system. Eur J Neurosci. 33:1563–1574.

Djuric U, Cheung AY, Zhang W, Mok RS, Lai W, Piekna A, Hendry JA, Ross PJ, Pasceri P, Kim DS, et al. 2015. MECP2e1 isoform mutation affects the form and function of neurons derived from Rett syndrome patient iPS cells. Neurobiol Dis. 76:37–45.

Englund C, Fink A, Lau C, Pham D, Daza RA, Bulfone A, Kowalczyk T, Hevner RF. 2005. Pax6, Tbr2, and Tbr1 are expressed sequentially by radial glia, intermediate progenitor cells, and postmitotic neurons in developing neocortex. J Neurosci. 25:247–251.

Ernst C. 2016. Proliferation and differentiation deficits are a major convergence point for neurodevelopmental disorders. Trends Neurosci. 39:290–299.

Fehr S, Bebbington A, Ellaway C, Rowe P, Leonard H, Downs J. 2011. Altered attainment of developmental milestones influences the age of diagnosis of rett syndrome. J Child Neurol. 26:980–987.

Feldman D, Banerjee A, Sur M. 2016. Developmental dynamics of Rett syndrome. Neural Plast. 2016:6154080.

Florio M, Huttner WB. 2014. Neural progenitors, neurogenesis and the evolution of the neocortex. Development. 141:2182–2194.

Goebbels S, Bormuth I, Bode U, Hermanson O, Schwab MH, Nave KA. 2006. Genetic targeting of principal neurons in neocortex and hippocampus of NEX-Cre mice. Genesis. 44: 611–621.

Gritti A, Parati EA, Cova L, Frolichsthal P, Galli R, Wanke E, Faravelli L, Morassutti DJ, Roisen F, Nickel DD, et al. 1996. Multipotential stem cells from the adult mouse brain proliferate and self-renew in response to basic fibroblast growth factor. J Neurosci. 16:1091–1100.

Guy J, Hendrich B, Holmes M, Martin JE, Bird A. 2001. A mouse Mecp2-null mutation causes neurological symptoms that mimic Rett syndrome. Nat Genet. 27:322–326.

Hardwick LJ, Ali FR, Azzarelli R, Philpott A. 2015. Cell cycle regulation of proliferation versus differentiation in the central nervous system. Cell Tissue Res. 359:187–200.

Haubensak W, Attardo A, Denk W, Huttner WB. 2004. Neurons arise in the basal neuroepithelium of the early mammalian telencephalon: a major site of neurogenesis. Proc Natl Acad Sci USA. 101:3196–3201.

Hendzel MJ, Wei Y, Mancini MA, Van Hooser A, Ranalli T, Brinkley BR, Bazett-Jones DP, Allis CD. 1997. Mitosis-specific phosphorylation of histone H3 initiates primarily within pericentromeric heterochromatin during G2 and spreads in an ordered fashion coincident with mitotic chromosome condensation. Chromosoma. 106:348–360.

Heng JI, Nguyen L, Castro DS, Zimmer C, Wildner H, Armant O, Skowronska-Krawczyk D, Bedogni F, Matter JM, Hevner R, et al. 2008. Neurogenin 2 controls cortical neuron migration through regulation of Rnd2. Nature. 455:114–118.

Hevner RF, Hodge RD, Daza RA, Englund C. 2006. Transcription factors in glutamatergic neurogenesis: conserved programs in neocortex, cerebellum, and adult hippocampus. Neurosci Res. 55:223–233.

Huppke P, Held M, Laccone F, Hanefeld F. 2003. The spectrum of phenotypes in females with Rett Syndrome. Brain Dev. 25: 346–351.

Kim KY, Hysolli E, Park IH. 2011. Neuronal maturation defect in induced pluripotent stem cells from patients with Rett syndrome. Proc Natl Acad Sci USA. 108:14169–14174.

Kishi N, Macklis JD. 2004. MECP2 is progressively expressed in post-migratory neurons and is involved in neuronal maturation rather than cell fate decisions. Mol Cell Neurosci. 27:306–321.

Kriaucionis S, Paterson A, Curtis J, Guy J, Macleod N, Bird A. 2006. Gene expression analysis exposes mitochondrial abnormalities in a mouse model of Rett syndrome. Mol Cell Biol. 26:5033–5042.

Lang M, Wither RG, Colic S, Wu C, Monnier PP, Bardakjian BL, Zhang L, Eubanks JH. 2014. Rescue of behavioral and EEG deficits in male and female Mecp2-deficient mice by delayed Mecp2 gene reactivation. Hum Mol Genet. 23:303–318.

Lange C, Huttner WB, Calegari F. 2009. Cdk4/cyclinD1 overexpression in neural stem cells shortens G1, delays neurogenesis, and promotes the generation and expansion of basal progenitors. Cell Stem Cell. 5:320–331.

Li H, Zhong X, Chau KF, Santistevan NJ, Guo W, Kong G, Li X, Kadakia M, Masliah J, Chi J, et al. 2014. Cell cycle-linked MeCP2 phosphorylation modulates adult neurogenesis involving the Notch signalling pathway. Nat Commun. 5:5601.

Li Y, Wang H, Muffat J, Cheng AW, Orlando DA, Loven J, Kwok SM, Feldman DA, Bateup HS, Gao Q, et al. 2013. Global transcriptional and translational repression in human-embryonic-stem-cell-derived Rett syndrome neurons. Cell Stem Cell. 13:446–458.

Lombardi LM, Baker SA, Zoghbi HY. 2015. MECP2 disorders: from the clinic to mice and back. J Clin Invest. 125: 2914–2923.

MacDonald JL, Roskams AJ. 2009. Epigenetic regulation of nervous system development by DNA methylation and histone deacetylation. Prog Neurobiol. 88:170–183.

Marchetto MC, Carromeu C, Acab A, Yu D, Yeo GW, Mu Y, Chen G, Gage FH, Muotri AR. 2010. A model for neural development

and treatment of Rett syndrome using human induced pluripotent stem cells. Cell. 143:527–539.

Miyata T, Kawaguchi A, Saito K, Kawano M, Muto T, Ogawa M. 2004. Asymmetric production of surface-dividing and non-surface-dividing cortical progenitor cells. Development. 131: 3133–3145.

Molyneaux BJ, Arlotta P, Menezes JR, Macklis JD. 2007. Neuronal subtype specification in the cerebral cortex. Nat Rev Neurosci. 8:427–437.

MuhChyi C, Juliandi B, Matsuda T, Nakashima K. 2013. Epigenetic regulation of neural stem cell fate during corticogenesis. Int J Dev Neurosci. 31:424–433.

Mullen RJ, Buck CR, Smith AM. 1992. NeuN, a neuronal specific nuclear protein in vertebrates. Development. 116:201–211.

Nagai K, Miyake K, Kubota T. 2005. A transcriptional repressor MeCP2 causing Rett syndrome is expressed in embryonic non-neuronal cells and controls their growth. Brain Res Dev Brain Res. 157:103–106.

Neul JL. 2012. The relationship of Rett syndrome and MECP2 disorders to autism. Dialogues Clin Neurosci. 14:253–262.

Noctor SC, Martinez-Cerdeno V, Ivic L, Kriegstein AR. 2004. Cortical neurons arise in symmetric and asymmetric division zones and migrate through specific phases. Nat Neurosci. 7:136–144.

Nomura Y. 2005. Early behavior characteristics and sleep disturbance in Rett syndrome. Brain Dev. 27(Suppl 1):S35–S42.

Okabe Y, Kusaga A, Takahashi T, Mitsumasu C, Murai Y, Tanaka E, Higashi H, Matsuishi T, Kosai K. 2010. Neural development of methyl-CpG-binding protein 2 null embryonic stem cells: a system for studying Rett syndrome. Brain Res. 1360:17–27.

Petazzi P, Akizu N, Garcia A, Estaras C, Martinez de Paz A, Rodriguez-Paredes M, Martinez-Balbas MA, Huertas D, Esteller M. 2014. An increase in MECP2 dosage impairs neural tube formation. Neurobiol Dis. 67:49–56.

Picker JD, Yang R, Ricceri L, Berger-Sweeney J. 2006. An altered neonatal behavioral phenotype in Mecp2 mutant mice. Neuroreport. 17:541–544.

Piton A, Gauthier J, Hamdan FF, Lafreniere RG, Yang Y, Henrion E, Laurent S, Noreau A, Thibodeau P, Karemera L, et al. 2011. Systematic resequencing of X-chromosome synaptic genes in autism spectrum disorder and schizophrenia. Mol Psychiatry. 16:867–880.

Pohodich AE, Zoghbi HY. 2015. Rett syndrome: disruption of epigenetic control of postnatal neurological functions. Hum Mol Genet. 24:R10–R16.

Skene PJ, Illingworth RS, Webb S, Kerr AR, James KD, Turner DJ, Andrews R, Bird AP. 2010. Neuronal MeCP2 is expressed at near histone-octamer levels and globally alters the chromatin state. Mol Cell. 37:457–468.

Smeets EE, Pelc K, Dan B. 2012. Rett syndrome. Mol Syndromol. 2:113–127.

Smrt RD, Eaves-Egenes J, Barkho BZ, Santistevan NJ, Zhao C, Aimone JB, Gage FH, Zhao X. 2007. Mecp2 deficiency leads to delayed maturation and altered gene expression in hippocampal neurons. Neurobiol Dis. 27:77–89.

Spitzer NC. 2006. Electrical activity in early neuronal development. Nature. 444:707–712.

Subramanian A, Tamayo P, Mootha VK, Mukherjee S, Ebert BL, Gillette MA, Paulovich A, Pomeroy SL, Golub TR, Lander ES, et al. 2005. Gene set enrichment analysis: a knowledge-based approach for interpreting genome-wide expression profiles. Proc Natl Acad Sci USA. 102:15545–15550.

Takahashi T, Nowakowski RS, Caviness VS Jr. 1995. The cell cycle of the pseudostratified ventricular epithelium of the embryonic murine cerebral wall. J Neurosci. 15:6046–6057.

Tanaka Y, Kim KY, Zhong M, Pan X, Weissman SM, Park IH. 2014. Transcriptional regulation in pluripotent stem cells by methyl CpG-binding protein 2 (MeCP2). Hum Mol Genet. 23: 1045–1055.

Telley L, Govindan S, Prados J, Stevant I, Nef S, Dermitzakis E, Dayer A, Jabaudon D. 2016. Sequential transcriptional waves direct the differentiation of newborn neurons in the mouse neocortex. Science. 351:1443–1446.

Tropea D, Giacometti E, Wilson NR, Beard C, McCurry C, Fu DD, Flannery R, Jaenisch R, Sur M. 2009. Partial reversal of Rett syndrome-like symptoms in MeCP2 mutant mice. Proc Natl Acad Sci USA. 106:2029–2034.

Tsankova N, Renthal W, Kumar A, Nestler EJ. 2007. Epigenetic regulation in psychiatric disorders. Nat Rev Neurosci. 8:355–367.

Tsujimura K, Abematsu M, Kohyama J, Namihira M, Nakashima K. 2009. Neuronal differentiation of neural precursor cells is promoted by the methyl-CpG-binding protein MeCP2. Exp Neurol. 219:104–111.

Tudor M, Akbarian S, Chen RZ, Jaenisch R. 2002. Transcriptional profiling of a mouse model for Rett syndrome reveals subtle transcriptional changes in the brain. Proc Natl Acad Sci USA. 99:15536–15541.

Turrero Garcia M, Chang Y, Arai Y, Huttner WB. 2016. S-phase duration is the main target of cell cycle regulation in neural progenitors of developing ferret neocortex. J Comp Neurol. 524:456–470.

Van Hooser A, Goodrich DW, Allis CD, Brinkley BR, Mancini MA. 1998. Histone H3 phosphorylation is required for the initiation, but not maintenance, of mammalian chromosome condensation. J Cell Sci. 111(Pt 23):3497–3506.

Yazdani M, Deogracias R, Guy J, Poot RA, Bird A, Barde YA. 2012. Disease modeling using embryonic stem cells: MeCP2 regulates nuclear size and RNA synthesis in neurons. Stem Cells. 30:2128–2139.